JACS
JOURNAL OF THE AMERICAN CHEMICAL SOCIETY
Communication
pubs.acs.org/JACS

Triggered "On/Off" Micropumps and Colloidal Photodiode

Vinita Yadav,† Hua Zhang,† Ryan Pavlick, and Ayusman Sen*

Department of Chemistry, The Pennsylvania State University, University Park, Pennsylvania 16802, United States

Supporting Information

ABSTRACT: We discuss a set of smart micropumps that sense their surrounding environment and respond accordingly. First we show that crystallites of a photoacid generator function as micropumps in the presence of UV light via diffusiophoresis and can be turned "on/off" in a controlled manner. The pump can be restarted multiple times simply by re-illumination. The electroosmotic component was distinguished from the diffusiophoretic component and compared. We also demonstrate patterning. Second, we show that a polymeric imine can also work as a micropump in acidic environment wherein the velocity can be controlled by controlling the pH and, in turn, the ion gradient; the highest velocities are achieved at the lowest pH. Finally, we combined the photoacid and polyimine pumps to create a colloidal photodiode, where we attain both spatial and temporal control over colloidal transport and obtain amplification along with rectification.

An important challenge in designing nano/micro-scale motors and pumps involves achieving directed transport to a precise destination.[1−8] Such fine-tuned motion is essential for complex functions in microfluidic chips, cargo delivery systems, and self-assembly applications. Further, it is also highly desirable that these pumps be capable of being turned on by a specific external signal. Here, we demonstrate autonomous micropumps based on simple acid−base- and photochemistry-induced ion gradients that result in spatio-temporal control of fluid flow. A few micropumps that cause fluid flow in response to specific fuels or chemical signals have been described previously.[9−15] These systems typically lack control since they cannot be readily turned off and on again.[16] Having an on/off switch is important for it allows the pump to respond to changes in the environment, which is useful for the design of sensors and logic gates.

We used a simple off-the-shelf photoacid generator (PAG) to demonstrate a UV-initiated pump with an "on/off" switch that can further be used for patterning. We then utilized the acid-catalyzed hydrolysis of a polymeric imine[17−20] to create a pump with pH regulated velocities. Finally, we utilized the combination of PAG and polyimine to create a source−drain-based "photodiode" that gives spatio-temporal control over colloidal mobility.

As shown in Figure 1, upon illumination of the solid photoacid generator, *N*-hydroxyphthalimide triflate (PAG-1), at wavelength 365 nm, it forms *N*-hydroxyphthalimide, and two ions: proton and triflate anion. The large difference in diffusion coefficients between the small cation and the large anion, establishes a diffusion-induced electric field pointing toward the

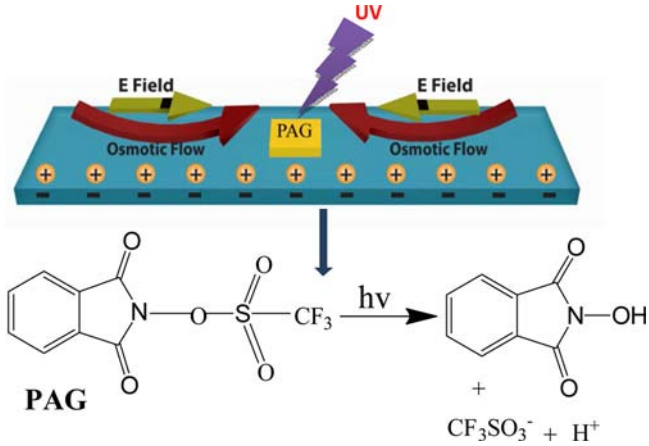

Figure 1. Schematic depiction of the PAG pumping mechanism. The negative surface charge of the glass creates a positive double layer, which in response to the generated ions causes an inward electroosmotic flow. The negatively charged tracers (S-PS particles) move opposite to the direction of the electric field, competing against the electroosmotic flow while the positively charged tracers (NH_2-PS particles) move along the electric field direction aided by the electroosmotic flow.

PAG that is responsible for the observed diffusiophoretic motion.

In an unbounded solution of a symmetrically charged binary electrolyte with a uniform concentration gradient ∇_c, the diffusiophoretic velocity of a charged particle, U, is given by[21]

$$U = \frac{\varepsilon kT}{2e\eta}\left[\left(\frac{D^+ - D^-}{D^+ + D^-}\right)\zeta_p - \frac{2kT}{Ze}\ln(1-\gamma^2)\frac{\nabla_c}{c_0}\right] \quad (1)$$

where D^+ and D^- are the diffusion coefficients of the cation and anion respectively, Z is the absolute value of the valences of the ions, e is the charge of an electron, k is the Boltzmann constant, T is the absolute temperature, ε is the dielectric permittivity of the solution, η is the viscosity of the solution, ζ_p is the zeta potential of the particle, $\gamma = \tanh(Ze\zeta_p/4kT)$, and c_0 is the bulk concentration of ions at the particle location, as if the particle was not there. The electroosmotic component is given by a similar equation, with the particle zeta potential replaced by the wall zeta potential.

The net velocities in our system result from the competition between the diffusiophoresis and the electroosmosis (Figure 1). With the proton diffusing faster ($D = 9.31 \times 10^{-5}$ cm^2/s) than the larger triflate anion (estimated $D = 1.38 \times 10^{-5}$ cm^2/s

Received: July 24, 2012
Published: September 12, 2012

   dx.doi.org/10.1021/ja307270d | J. Am. Chem. Soc. 2012, 134, 15688−15691

assuming a sphere), a local electric field is set up pointing inward. Owing to the electric double layer on the negatively charged sodium borosilicate glass slide, an electroosmotic flow is generated, which is also inward in the direction of the local electric field. Positively charged tracers (amino-functionalized polystyrene particles NH_2-PS) were observed to move toward the photoacid, aided by both the diffusiophoretic and electroosmotic flows, attaining an average velocity of 7.2 ± 2.4 μm/s. The negatively charged tracers (sulfate functionalized polystyrene particles S-PS and carboxylate-functionalized polystyrene particles HOOC-PS) on the other hand, move in the direction of the diffusiophoretic flows, out-winning the electroosmotic flow, owing to their higher zeta potential in comparison to that of the glass.[22,25] In our system, the pH changes from 6.8 to 2 and the ionic strength changes from 10^{-6} to 10^{-3} M. *In this range*, the zeta potential of glass and involved tracers are as follow: glass, −30 to −60 mV;[22] NH_2-PS, ∼+55 mV;[23] S-PS, −100 to −180 mV;[24] HOOC-PS, −120 to −160 mV,[25] the exact value depending on the ionic strength and pH. The S-PS particles attained an average velocity of 4.8 ± 1.3 μm/s, and that for HOOC-PS particles was calculated to be 4.1 ± 0.9 μm/s. Note that all the reported velocities were measured close to the wall (glass surface). As expected, due to fluid continuity, the direction of motion is reversed when observing particles several hundred micrometers above the wall. The motion ceases when UV light is turned off but can be reinitiated upon re-illumination. Only Brownian diffusion is observed in the absence of UV light. Another control was performed by first exhausting the photoacid by prolonged UV illumination, until it no longer produces protons (no measurable change in pH). Here again, no powered motion was observed even under illumination. Hence, the role of a thermal gradient in causing flow can be ruled out. Figure 2 displays the tracer particle distributions without UV and after 1 min of UV irradiation.

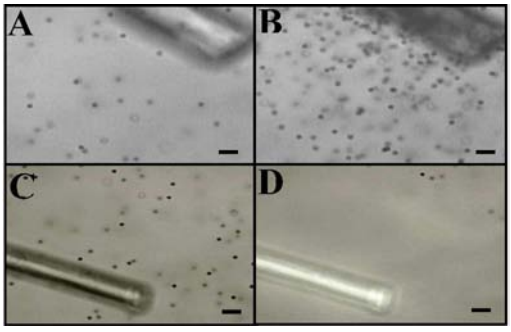

Figure 2. Optical microscope images of particle (2 μm) motion. (A,B) Distribution of the positively charged tracers (NH_2-PS) around the photoacid (PAG-1) microcrystallites with UV off (control) and after 1 min of UV illumination, respectively. (C,D) The same for the negatively charged tracers (S-PS). See SI videos S1 and S2. Scale bar (bottom right) is 10 μm.

In order to separate the diffusiophoretic and electroosmotic components, the same experiments were performed on a polystyrene surface, which has minimal surface charge. The particles (2 μm) were tracked over a 6 s period using PhysVis software. The velocities of the positively charged tracers were impeded in the absence of the aiding electroosmotic force (average velocity = 4.0 ± 0.4 μm/s), while those of the negatively charged tracers were enhanced due to the absence of the opposing electroosmotic force (S-PS particle, average velocity = 7.9 ± 1.1 μm/s; HOOC-PS particle, average velocity = 6.6 ± 0.3 μm/s), both by a factor of ∼2. Thus, the estimated contributions of diffusiophoretic and electroosmotic components of velocity are approximately equal (velocity distribution histograms, Supporting Information (SI), Figure S1).

As shown in Figure 3, diffusiophoretic pumping by PAG upon illumination can be employed for patterned self-assembly

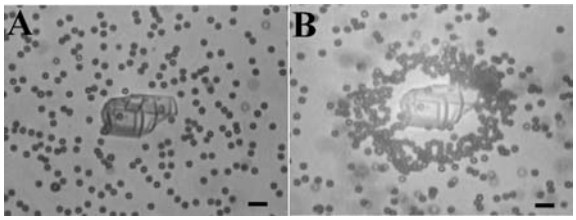

Figure 3. Patterns induced by PAG pumping. (A) Control image, NH_2-PS particle distribution around a single photoacid crystallite with UV off. (B) Self-assembled NH_2-PS particle pattern with UV on. Scale bar (bottom right) is 6 μm.

of tracer particles (2 μm) (SI video S3). The result encouraged us to utilize the photoacid to induce guided motion through microchannels to achieve patterning at the micrometer scale using photoinduced ion gradients. We used a laser printer for designing our pattern on polyacrylate surface (see SI and Figure 4). *N*-Hydroxy-5-norbornene-2,3-dicarboximide perfluoro-1-

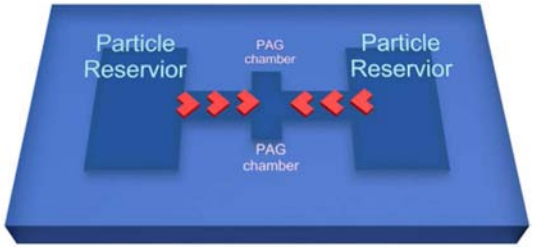

Figure 4. Schematic depiction of the pattern. The pump pulls the NH_2-PS particles out from the large reservoirs (10×10 mm^2) into the microchannels (4×1 mm^2), toward the PAG chambers (1×1 mm^2) on either side of the channel.

butanesulfonate, PAG-2, was used for this experiment due to its granular morphology and its ease of packing in the 1×1 mm^2 compartment within the pattern. Upon UV illumination, tracers (NH_2-PS) were pulled out of the large reservoirs and were made to follow the designed microchannel in the pattern (SI video S4). When the UV was switched off, the particle motion relaxed and picked up again as the UV was turned back on. Thus, the motion can be initiated and stopped repeatedly.

The acid-catalyzed hydrolysis of a polymeric imine, poly(4-formylphenyl acrylate) aniline Schiff base (PFA-S) film cast on a glass slide also results in diffusiophoretic pumping, only this time with the direction of the local electric field reversed due to the higher diffusivity of the anion (D_{Cl^-} = 2.032 × 10^{-5} cm^2/s) relative to the much larger cation (Figure 5; SI videos S5 and S6). Accordingly, the movement of the tracers was observed to be reversed with the negative HOOC-PS tracers moving inward competing against the electroosmotic component and the positively charged NH_2-PS particles moving outward, aided by the electroosmotic component.

Figure 6 shows optical images of the pumping by PFA-S film. In accordance with eq 1, the velocities attained by the tracer

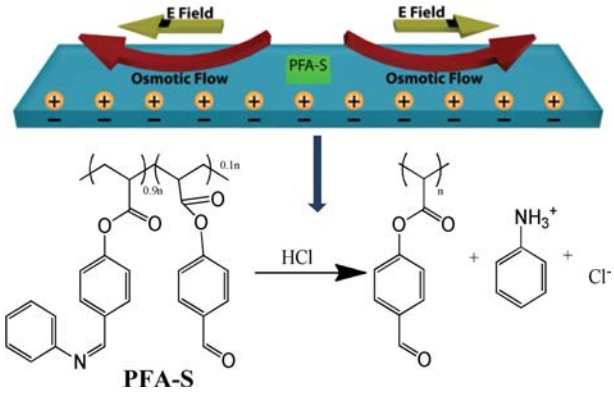

Figure 5. Schematic depiction of PFA-S pumping mechanism. The local electric field points outward, away from the polymer film, and the negatively charged tracers, HOOC-PS particles, move inward, toward the film.

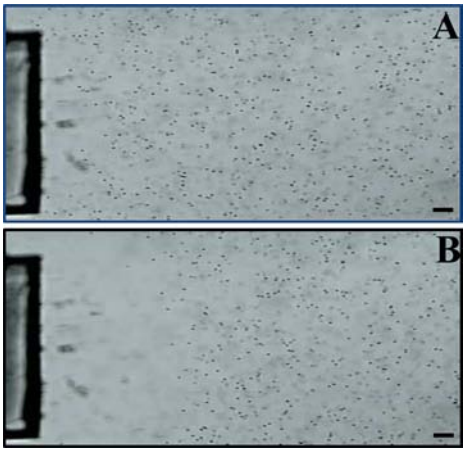

Figure 6. Optical microscope images of PFA-S film pumping away HOOC-PS tracers (6 μm). (A) Image taken 0 s after exposure to 1 M HCl in deionized water at 25 °C, and (B) 1200 s after exposure. Scale bar (bottom right) is 30 μm.

particles should depend on the concentration gradient of the formed electrolytes. Accordingly, varying concentrations of HCl were introduced into the PFA-S system and the HOOC-PS particle velocities measured for each concentration. As expected, the particle velocities showed an increase with decreasing pH reaching an average velocity of 3.2 ± 0.8 μm/s in 1 M HCl (Figure 7). The particle velocities were measured at distances from 100 to 200 μm away from the pump, 0 to 62.5 s after exposure to acid. The velocity distribution histograms at each proton concentration, over the specified range of distance and time, are shown in Figure 7. The ionic strength at each acid concentration (1, 0.1, and 0.01 M HCl) was kept the same as that at 1 M, to avoid any changes to the electric double layer.

Further, as expected of a diffusiophoretic pump, the pumping velocities also show a dependence on the distance from the pump source. Average particle velocity changes as a function of distance for the PFA-S pump over the time period of 0 to 25 s after exposure to 1 M HCl at 25 °C (velocity distribution histograms, SI, Figure S2). The PFA-S pump is capable of providing minimum average pumping velocities of 2.0 ± 0.6 μm/s at distances over 1 mm from the pump.

Encouraged by the above results, we decided to combine the two individual pumps to create a source−drain-based colloidal

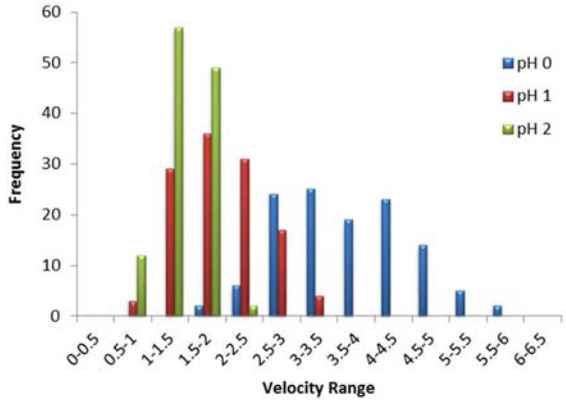

Figure 7. Velocity distribution histograms of HOOC-PS tracers as a function of the acid concentration for the PFA-S pump.

photodiode which uses UV as the input to regulate the direction and speed of particle transport. For this experiment, the PAG and the PFA-S were cast into separate films, about 300 μm away from each other to create an emitter (PAG, proton generator)−collector (PFA-S, proton consumer) system (Figure 8). The experiments were performed on glass surface

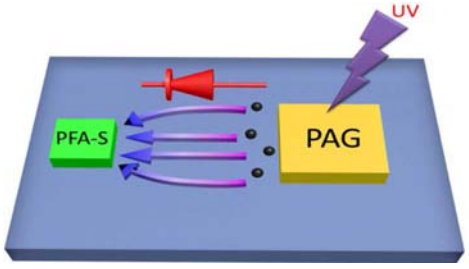

Figure 8. Schematic depiction of source (PAG)−drain (PFA-S)-based colloidal photodiode indicating both the rectification and amplification of movement of S-PS particles.

using S-PS tracers (2 μm) owing to their high zeta potential and desired direction of motion: away from PAG and toward PFA-S. This push−pull mechanism results in rectification of particle motion.

Before each experiment, a control video was recorded with UV lamp off. The tracers show no directional movement, only Brownian motion was observed. Upon UV illumination, the PAG initiates the diffusiophoretic motion pushing the negatively charged tracers away in all directions (SI video S7). When the acid formed by the photolysis of PAG reaches the PFA-S film, it starts imine hydrolysis; the PFA-S film then actively pulls the tracers precisely toward itself, and further enhances the tracer velocities. As a result, the particle velocities *in between* the source and the drain were observed to be much faster than those on opposite sides of either of them. Thus, upon illumination, the particles began moving away from the PAG slowly and their velocities steadily increased as they approached the drain; PFA-S. Moreover, the velocities in between the source and drain were time-dependent owing to the delay in the PFA-S's hydrolysis which depends on the diffusion of the acid from the illuminated PAG. Figure 9 depicts the spatial and temporal control achieved using the source−drain setup, with the particles reaching a maximum average velocity of 3.9 μm/s. Effectively, our colloidal photodiode is capable of amplifying the velocity, as well as directing the

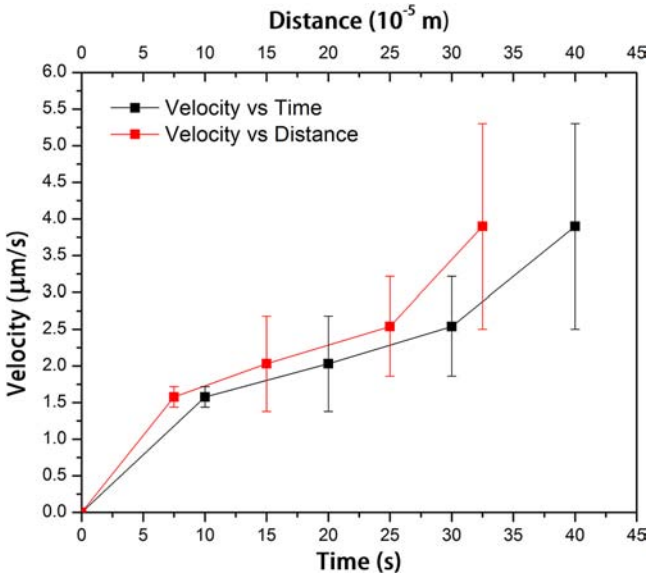

Figure 9. Spatial and temporal regulation of velocity (S-PS particles) attained using the source−drain photodiode. Distance is measured from edge of the PAG and time is measured from when the UV is turned on. For velocity vs time plot, distance = 150 μm; for velocity vs distance plot, time = 20 s.

particle flow in one direction, without introducing a third "base/gate" terminal as required by a typical transistor. This opens the door to creating more complex colloidal logic systems.

In conclusion, this Communication describes a set of smart self-powered microscale pumps capable of converting chemical/photochemical energy directly into mechanical motion. The phototriggered pump can be turned on and off repeatedly. We also demonstrate the design of a colloidal photodiode. This opens up further avenues to amplify and attain spatio-temporal control over colloidal transport.

■ ASSOCIATED CONTENT

Ⓢ Supporting Information

Materials, experimental procedures, velocity histograms, and videos S1−S7 (files ja307270d_si_002.avi through ja307270d_si_008.avi, respectively). This material is available free of charge via the Internet at http://pubs.acs.org.

■ AUTHOR INFORMATION

Corresponding Author

asen@psu.edu

Author Contributions

†V,Y. and H.Z. contributed equally to this work.

Notes

The authors declare no competing financial interest.

■ ACKNOWLEDGMENTS

We gratefully acknowledge funding by the National Science Foundation (DMR-0820404, CBET-1014673).

■ REFERENCES

(1) Paxton, W. F.; Sundararajan, S.; Mallouk, T. E.; Sen, A. *Angew. Chem., Int. Ed.* **2006**, *45*, 5420.
(2) Hong, Y.; Velegol, D.; Chaturvedi, N.; Sen, A. *Phys. Chem. Chem. Phys.* **2010**, *12*, 1423.
(3) Sanchez, S.; Pumera, M. *Chem. Asian J.* **2009**, *4*, 1402.
(4) Mei, Y. F.; Solovev, A. A.; Sanchez, S.; Schmidt, O. G. *Chem. Soc. Rev.* **2011**, *40*, 2109.
(5) Wang, J. *ACS Nano* **2009**, *3*, 4.
(6) Wang, J.; Manesh, K. M. *Small* **2010**, *6*, 338.
(7) Mirkovic, T.; Zacharia, N. S.; Scholes, G. D.; Ozin, G. A. *Small* **2010**, *6*, 159.
(8) Ebbens, S. J.; Howse, J. R. *Soft Matter* **2012**, *8*, 3077.
(9) Jun, I. K.; Hess, H. *Adv. Mater.* **2010**, *22*, 4823.
(10) Kline, T. R.; Paxton, W. F.; Wang, Y.; Velegol, D.; Mallouk, T. E.; Sen, A. *J. Am. Chem. Soc.* **2005**, *127*, 17150.
(11) Ibele, M. E.; Wang, Y.; Kline, T. R.; Mallouk, T. E.; Sen, A. *J. Am. Chem. Soc.* **2007**, *129*, 7762.
(12) Pavlick, R. A.; Sengupta, S.; McFadden, T.; Zhang, H.; Sen, A. *Angew. Chem., Int. Ed.* **2011**, *50*, 9374.
(13) Zhang, H.; Yeung, K.; Robbins, J. S.; Pavlick, R. A.; Wu, M.; Liu, R.; Sen, A.; Phillips, S. T. *Angew. Chem., Int. Ed.* **2012**, *51*, 2400.
(14) Smith, E. J.; Xi, W.; Makarov, D.; Monch, I.; Harazim, S.; Quinones, V. A. B.; Schmidt, C. K.; Mei, Y.; Sanchez, S.; Schmidt, O. G. *Lab Chip* **2012**, *12*, 1917.
(15) Solovev, A. A.; Sanchez, S.; Mei, Y.; Schmidt, O. G. *Phys. Chem. Chem. Phys.* **2011**, *13*, 10131.
(16) Solovev, A. A.; Smith, E. J.; Bof Bufon, C. C; Sanchez, S.; Schmidt, O. G. *Angew. Chem., Int. Ed.* **2011**, *50*, 10875.
(17) Tauk, L.; Schröder, A. P.; Decher, G.; Giuseppone, N. *Nat. Chem.* **2009**, *1*, 649.
(18) Deng, G.; Tang, C.; Li, F.; Jiang, H.; Chen, Y. *Macromolecules* **2010**, *43*, 1191.
(19) Gu, J.; Cheng, W.-P.; Liu, J.; Lo, S.-Y.; Smith, D.; Qu, X.; Yang, Z. *Biomacromolecules* **2007**, *9*, 255.
(20) Wang, C.; Wang, G.; Wang, Z.; Zhang, X. *Chem. Eur. J.* **2011**, *17*, 3322.
(21) Anderson, J. L. *Annu. Rev. Fluid Mech.* **1989**, *21*, 61.
(22) Gu, Y.; Li, D. *J. Colloid Interface Sci.* **2000**, *226*, 328.
(23) Delair, T.; Meunier, F.; Elaissari, A.; Charles, M. H.; Pichot, C. *Colloids Surf. A: Physiochem. Eng. Aspects* **1999**, *153*, 341.
(24) Bastos, D.; De Las Nieves, F. J. *Prog. Colloid Polym. Sci.* **1993**, *93*, 37.
(25) Gracia-Salinas, M. J.; Romero-Cano, M. S.; De Las Nieves, F. J. *Polym. Colloid Solid Particles* **2000**, *115*, 112.